Novel Electrically Conductive and Ferromagnetic Composites of Poly(aniline-*co*-aminonaphthalenesulfonic acid) with Iron Oxide Nanoparticles: Synthesis and Characterization

Kakarla Raghava Reddy,[1] Kwang-Pill Lee,[1,2] Anantha Iyengar Gopalan[1,2]

[1]*Department of Chemistry Graduate School, Kyungpook National University, Daegu 702-701, South Korea*
[2]*Nanomaterials Laboratory, Nano Practical Application Center, Daegu 704-230, South Korea*

Received 13 April 2006; accepted 8 April 2007
DOI 10.1002/app.26601
Published online 8 July 2007 in Wiley InterScience (www.interscience.wiley.com).

ABSTRACT: Nanocomposites of iron oxide (Fe_3O_4) with a sulfonated polyaniline, poly(aniline-*co*-aminonaphthalenesulfonic acid) [SPAN(ANSA)], were synthesized through chemical oxidative copolymerization of aniline and 5-amino-2-naphthalenesulfonic acid/1-amino-5-naphthalenesulfonic acid in the presence of Fe_3O_4 nanoparticles. The nanocomposites [Fe_3O_4/SPAN(ANSA)-NCs] were characterized by transmission electron microscopy (TEM), scanning electron microscopy (SEM), X-ray diffraction (XRD), Fourier transform infrared (FTIR) spectroscopy, elemental analysis, UV–visible spectroscopy, thermogravimetric analysis (TGA), superconductor quantum interference device (SQUID), and electrical conductivity measurements. The TEM images reveal that nanocrystalline Fe_3O_4 particles were homogeneously incorporated within the polymer matrix with the sizes in the range of 10–15 nm. XRD pattern reveals that pure Fe_3O_4 particles are having spinel structure, and nanocomposites are more crystalline in comparison to pristine polymers. Differential thermogravimetric (DTG) curves obtained through TGA informs that polymer chains in the composites have better thermal stability than that of the pristine copolymers. FTIR spectra provide information on the structure of the composites. The conductivity of the nanocomposites (~ 0.5 S cm^{-1}) is higher than that of pristine PANI ($\sim 10^{-3}$ S cm^{-1}). The charge transport behavior of the composites is explained through temperature difference of conductivity. The temperature dependence of conductivity fits with the quasi-1D variable range hopping (quasi-1D VRH) model. SQUID analysis reveals that the composites show ferromagnetic behavior at room temperature. The maximum saturation magnetization of the composite is 9.7 emu g^{-1}. © 2007 Wiley Periodicals, Inc. J Appl Polym Sci 106: 1181–1191, 2007

Key words: copolymerization; sulfonated polyanilines; Fe_3O_4 nanoparticles; nanocomposite; conductivity; ferromagnetic property

INTRODUCTION

Conducting polymers (CPs) are unique class of materials that exhibit electrical and optical properties of metals or semiconductors.[1] They offer great prospects for practical applications because of their unparalleled architectural diversity and flexibility, inexpensiveness, and ease of synthesis. To some extent, the field of organic conductors has evolved from a simple science into a resource for new technologies. CPs find suitability for applications as chemical and biological sensors, electrochromic devices, secondary batteries, electrostatic discharge protection, field-effect transistors, integrated circuits, light emitting diodes, solar cells, and microcavity resonance.[2,3]

The advent of nanostructuring of CPs and their utilities for device applications has necessitated further interest in this dynamic field. The properties of these polymers mainly depend on their nanostructures and morphologies that are controlled by the synthesis. Among CPs, polyaniline (PANI) is probably the most widely studied because it has a broad range of tunable properties derived from its structural flexibility. PANI has few advantages like good environmental stability, ease of preparation in aqueous solution and organic solutions, unique optical, electrical, electrochemical, electrochemomechanical properties, and reversible nonredox doping/dedoping process based on acid/base reactions.[4–6] Not withstanding the immense potentials for commercial viability, the applications of PANI remain quite below the expected target due to rigidity of the PANI backbone, causing insolubility in common solvents and infusibility at traditional melt-processing temperatures. The industrial demands for applications of PANI have led to prepare soluble and processable PANI.

Correspondence to: K. P. Lee (kplee@knu.ac.kr).
Contract grant sponsor: Korean Research Foundation; contract grant number: KRF-2006-J02402.

Journal of Applied Polymer Science, Vol. 106, 1181–1191 (2007)

Newer methods and derivatives like sulfonated PANs (SPANs), phosphonic acid doped PANI, emulsion polymerization using surfactant, and enzymatic synthesis of PANI/sulfonated polystyrene complex were tried to prepare soluble PANI.[7–9] In the process of improving processability of PANI, derivatives of PANI, and blends or organic-based composites have also been prepared.[10–12] Few reports revealed that conductivity and solubility of PANI could be improved by doping PANI with organic dopants like *p*-toluenesulfonic, dodecylbenzenesulfonic, camphor sulfonic, and poly(styrene) sulfonic acids.[6] The enhancement in the solubility has been attributed to the presence of organic moieties, which promote compatibility of PANI polymer with the solvent. Also, PANI derivatives were prepared to improve properties of PANI. Alkyl, alkoxy, methoxy, sulfonic, alkoxysulfonic, or carboxylic acid derivatives of PANI have been prepared.[6]

Among other PANI derivatives, SPANs received greater attention because of the advantageous properties like self-doping, thermal stability, optical properties, solubility, and better processability over PANI.[8] SPAN contains ionizable and negatively charged sulfonic acid groups. As a result, self-doping and consequent additional stability are in-built in SPAN. SPANs can be generally prepared by two methods: (1) posttreatment of base form of PANI (e.g., emeraldine base or leucoemeraldine base) with a sulfonating agent, and (2) homopolymerization of sulfonated anilines or the copolymerization of aniline with other sulfonated anilines. Copolymerization of aniline with aminobenzenesulfonic acid could produce materials with different structures and properties. SPANs prepared by copolymerization possess better thermal stability over SPANs having a similar degree sulfonation but prepared by the post-sulfonation of PANI.[6] Composites of SPANs have potential applications in rechargeable batteries, light-emitting diodes, sensors, junction devices, electromagnetic shielding materials, corrosion protection, and enzymatic activity.[6,7,12]

Organic–inorganic nanocomposites with different combinations of the two components have attracted significant academic and technological attention as they have interesting physical properties and potential applications.[13] Composites of CPs prepared by the incorporation of metal (e.g., Au, Pt, Ag, Pd or Cu) or semiconductor (CdS or CdTe) or metal oxide (Fe_3O_4, V_2O_5, TiO_2, or SiO_2) nanoparticles into CPs attract substantial research efforts, as these hybrid materials possess new catalytic, electronic, or optoelectronic functionalities.[13–16] Metallic or semiconductor nanoparticles were incorporated into polypyrrole or PANI through the electronic interactions between the nanoparticles and the polymer matrices. The layer of CP over metal nanoparticles protects them from corrosion and gives longer performance. It has been shown that the electrocatalytic properties of nanoparticles are enhanced by the conductive environment provided by the polymer matrices, while the conductivity of the hybrid system is improved in the presence of metal nanoparticles embedded into the polymer matrix.[17] Athawale and Bhagwat have synthesized a PANI-Cu nanocomposite and showed that composites have higher electrical conductivity than pure PANI.[18] Also, they reported that the composite can be used as a catalyst for the conversion of alkenes to ketenes or aldehydes in a single step. Somani et al.[19] synthesized PANI-TiO_2 composites by *in situ* deposition method and analyzed the piezoresistive functions. Gurunathan and Trivedi[20] studied the effect of photoconducting TiO_2 on the thermal stability and found that the PANI-TiO_2 composite did not lose its color until 270°C. Ficiglu et al.[21] reported that PANI-Pt composite has good catalytic activity as the electronic charges can be shuttled between PANI and Pt particles. Hence, there has been an increasing interest in the fabrication of these types of composites with enhanced optical, electrical, and magnetic properties.

Iron oxide (Fe_xO_y, Fe_3O_4/Fe_2O_3) nanoparticles have received great deal of attention because of their unique electrical, magnetic, optical, catalytic, and biological properties as well extensive applications in diverse areas.[22] Fe_3O_4 exhibits most interesting properties due to existence of Fe cations in two valence states: the bivalent Fe^{2+} ion and the trivalent Fe^{3+} ions (Fe_3O_4 can be written in the form $[Fe^{3+}]_A[(Fe^{2+},Fe^{3+})]_BO_4$, in which *A* represents tetrahedral sites and *B* for octahedral sites). Fe_3O_4 fluids find uses in biomedical fields, catalysis, magnetic data storage, photonic crystals, and spin electronic devices, because of intrinsic ferromagnetic nature.[22,23] However, nanometer-sized Fe_3O_4 particles aggregate easily due to anisotropic dipolar attractions. It becomes important to prevent such an aggregation. Coating of CPs on Fe_3O_4 nanoparticles can enhance compatibility with organic ingredients, reduce susceptibility to leaching, and probably avoid aggregation.

Magnetic composite materials comprise a new generation of multifunctional materials that combine the properties of conventional polymers and magnetic materials (ferri, and/or ferromagnetic particles mixed or embedded in a matrix) and the materials are classified as ''magneto-polymeric materials.'' These materials can be prepared by judicious combination of a magnetite material with a soluble polymer. Magnetic–electric and magnetic–optic properties and other combinations are expected because of the interaction between the magnetization and electric polarization. CPs such as PANI or polypyrrole shows magnetic behavior because of its high spin

density. Composites consisting of CPs and Fe_xO_y/ferrite are known as magnetoelectric materials.

Gangopadhyay and De[24] prepared the polypyrrole–ferric oxide nanocomposite in the presence of stable colloidal ferric oxide and reported the conductivity of composite. However, magnetic properties were not reported.[24] Butterworth et al.[25] reported the preparation of a composite through oxidatively deposited polypyrrole on silica-coated-Fe_3O_4 nanoparticles using aqueous oxidants H_2O_2/Fe^{3+}/HCl and $(NH_4)_2S_2O_8$. However, the conductivity of the resultant composite ($\sim 10^{-3}$ S cm^{-1}) was considerably lower than that of pristine polypyrrole. Magnetic saturation of the composite has been reported to be low due to the presence of silica. Chen et al.[26] used emulsion polymerization through polymerization of pyrrole in the presence of Fe_3O_4 particles and sodium dodecyl sulfate as surfactant. Aphesteguy and Jacobo[27] prepared PANI-Fe_3O_4 nanocomposite through polymerization of aniline in the absence of external oxidant. Mixture of iron(II) and iron(III) compounds were used as oxidants to polymerize aniline to PANI and form Fe_3O_4 particles in a single step, and conductivity of the composite was around 10^{-4} S cm^{-1}. Peng and coworkers[28] prepared the Fe_3O_4-crosslinked PANI nanocomposite with a core–shell structure by using formaldehyde as crosslinking agent. They also prepared Fe_3O_4-PANI nanoparticles with core–shell structure by *in situ* polymerization[29] and the composite had a low conductivity of $\sim 10^{-5}$ S cm^{-1}. Polymerization of aniline using a mixture of $FeCl_2$ and $FeCl_3$ as oxidants and subsequent treatment with aqueous KOH solution resulted in iron oxide-PANI composite.[30] Zhu et al.[31] prepared PANI-iron nanocomposite by cryomilling.

Recently, composites of PANI with metal ferrites have been reported.[32–35] Metal ferrites have general formula $MO{\cdot}Fe_2O_3$ or $MO{\cdot}Fe_3O_4$, where M is an element in a bivalent state, e.g., M^{2+} = Fe^{2+}, Ni^{+2}, Mn^{+2}, Zn^{+2}, etc., or a combination of them. Li et al.[32] fabricated core–shell composite of PANI with NiZn ferrite ($Ni_{0.5}Zn_{0.5}Fe_2O_4$) by microemulsion polymerization. The resulting composite showed a low conductivity (10^{-4} S cm^{-1}) and a magnetic saturation (0.76 emu g^{-1}). Li et al.[33,34] synthesized composites of PANI with $LiNi_{0.5}La_{0.02}Fe_{1.98}O_4$ ferrite/$LiNi_{0.5}Sm_{0.08}Fe_{1.92}O_4$ by an *in situ* polymerization. However, electrical conductivity of the resulting composites was not reported. Yavuz et al.[35] synthesized MnZn ferrite/NiMnZn ferrite-PANI composites by oxidative as well as electrochemical polymerization. However, the sizes of the composite particles were not reported. However, reports on the preparation and properties of the composites of SPANs with Fe_3O_4 nanoparticles are scarce. Further, a comprehensive report on the conductivity and magnetic properties of SPAN/Fe_3O_4 composite would provide basis for many of the applications such as wave guiders, transducers, sensors, etc. Such composite materials have special interest because of the possible optoelectromagnetic properties.

The present investigation deals with the synthesis of composites of poly(aniline-*co*-5-amino-2-naphthalenesulfonic acid)/poly(aniline-*co*-1-amino-5-naphthalenesulfonic acid) [designated as SPAN(ANSA)] with Fe_3O_4 nanoparticles by chemical oxidative copolymerization of mixture of aniline and a SPAN. Thermal, electrical, and magnetic properties of the Fe_3O_4/SPAN(ANSA) composites are investigated.

EXPERIMENTAL

Chemicals

Aniline (reagent grade, Oriental) was distilled under reduced pressure and stored below 0°C. 5-Amino-2-naphthalenesulfonic acid (ANSA-**A**) and 1-amino-5-naphthalenesulfonic acid (ANSA-**B**) were purchased from Aldrich, USA. Other reagents, iron(II) chloride tetra hydrate, iron(III) chloride hexahydrate, ammonium peroxydisulfate (APS), ammonium hydroxide, hydrochloric acid, and methanol of analytical grade were used without further purification. Milli-Q purified water was used for all the experiments.

Synthesis of Fe_3O_4 nanoparticles

Magnetic nanoparticles, Fe_3O_4, were synthesized by coprecipitating Fe^{+2} and Fe^{3+} ions by ammonia solution. $FeCl_2{\cdot}4H_2O$ (0.158 g) and $FeCl_3{\cdot}6H_2O$ (0.268 g) were dissolved in 45 mL of deionized water. Aqueous ammonia (1.2 mL; 28 wt %) was added into the solution of mixed iron salts, and the solution was purged with N_2 gas. Reaction was allowed to proceed for 1.5 h with stirring. A black precipitate was obtained. The precipitate was removed by centrifugation at 4000 rpm for 30 min and washed several times with distilled water and ethanol. The Fe_3O_4 particles thus obtained were dried in a vacuum oven for 6 h.

Synthesis of Fe_3O_4/SPAN(ANSA) nanocomposites

Nanocomposites, Fe_3O_4/SPAN(ANSA), were prepared using ANSA-**A** and ANSA-**B**. Fe_3O_4/SPAN(ANSA) nanocomposites were prepared through chemical oxidative copolymerization of aniline and ANSA-**A** or ANSA-**B** in the presence of Fe_3O_4 nanoparticles. A typical procedure for the synthesis of the Fe_3O_4/SPAN(ANSA)-NCs is described.

Fe_3O_4 nanoparticles (a definite amount) were added to 80 mL of aqueous 0.1*M* HCl solution containing aniline (0.1*M*) and ANSA-**A** (0.1*M*) (with a molar ratio of 1 : 1) and stirred under ultrasonic irra-

diation with a high-intensity ultrasonic probe with a power output of 700 W for 30 min. Diluted HCl was added here to solubilize the monomers. Also, HCl is one of the strongest dopants for the polymerization of aniline or its derivatives, and thus it can enhance the electrical conductivity for the resulting polymers or composites.[6,36,37] Subsequently, 20 mL of APS solution (0.2*M*) in 0.1*M* HCl was added dropwise to the aforementioned mixture at a rate of one drop for every 3 s at 3°C over a period of 20 min. Sonication was continued for 2 h and then the reaction mixture was stirred for 24 h. A dark-green precipitate was obtained. The precipitate was washed with an excess of distilled water and methanol, until the filtrate was colorless to remove the oxidant and oligomers, and dried in vacuum for 12 h. The nanocomposite thus obtained is designated as Fe_3O_4/SPAN(ANSA-**A**)-NC. In a similar way, Fe_3O_4/SPAN(ANSA-**B**)-NC was prepared using ANSA-**B** and aniline in the presence of Fe_3O_4 nanoparticles. For the comparative purpose, pristine SPAN(ANSA) copolymers were synthesized by performing experiments as similar to the preparation of Fe_3O_4/SPAN(ANSA-**A** or **B**)-NCs, but in the absence of Fe_3O_4 particles. Also, for a comparative purpose, pristine PANI was prepared without ANSA-**A** or **B** and Fe_3O_4 particles under similar conditions.

To investigate the structural, electrical, and magnetic properties of the nanocomposites, the Fe_3O_4/SPAN(ANSA-**A** or **B**) composite was stirred with 3 wt % ammonium hydroxide for 48 h to obtain the neutralized form of the Fe_3O_4/SPAN(ANSA) composite. The composites were isolated by filtration and washed several times with distilled water and methanol and dried at vacuum. The composites neutralized likewise are designated as Fe_3O_4/SPAN(ANSA-EB-**A**) and Fe_3O_4/SPAN(ANSA-EB-**B**), where EB states for emeraldine base form of the polymer.

To study the influence acidic solutions (0.1*M* HCl) on Fe_3O_4 and on monomers of aniline polymerization process, experiments were performed without the presence of APS, an external oxidizing agent. It is well known that iron(III) compounds (i.e., $FeCl_3$) can oxidize aniline or its derivatives to result in the formation of corresponding polymers.[38,39] If Fe^{3+} is formed by dissolution of Fe_3O_4 in 0.1*M* HCl, aniline monomers would have been polymerized with the development of green color on the walls of glass vessel. Since such changes were not observed, we presume that $FeCl_3$ is not formed. This study demonstrates that Fe_3O_4 is stable in diluted acidic solutions of aniline monomers, and the self-induced polymerization of aniline monomers is not possible on Fe_3O_4-SPAN composites without using APS. Hence, we conclude that Fe_3O_4 does not initiate polymerization of aniline monomers in diluted acidic solutions. Polymerization takes place only in the presence of APS.

Instrumental analysis

Fourier transform infrared (FTIR) spectra were recorded on a Bruker IFS 66v FTIR spectrometer using KBr pellets. Ultraviolet–visible (UV-vis) optical absorption spectra were recorded on Beckman UV-vis (DU7500) spectrophotometer with quartz cuvettes (0.2 cm) and in *N*-methylpyrrolidone (NMP) as the solvent. Elemental analysis was performed using a Carlo Erba 1106 elemental analyzer. The morphology and particle size measurements were made for Fe_3O_4 nanoparticles and composites by using transmission electron microscopy (TEM). The sample for TEM observation was prepared by the following procedure: Powder of the composite was dispersed in NMP through ultrasonication, and then the dispersion was dropped on a copper grid to observe the morphology of composite particle by using Phillips CM-30 TEM with an accelerating voltage of 100 kV. The particles in morphology were measured using a scale bar in the micrographs. The morphology of composites was evaluated by scanning electron microscopy (SEM JSM-6700 F, JEOL). Fine-powdered composite samples were deposited onto a silicon wafer and dried under nitrogen stream followed by sputtering with gold. SEM images were taken at an accelerating voltage of 25 kV. Thermal stability (TG-DTG) of composites and polymers were made using a Dupont 9900/2100 thermogravimetric analysis (TGA) at a heating rate of 10°C/min under a nitrogen atmosphere over a temperature range of 30–800°C. X-ray diffraction (XRD) patterns of Fe_3O_4 and Fe_3O_4/SPAN(ANSA)-NCs and polymers were recorded using Rigaku D/MAX 2550 V diffractometer with Nickel filtered using Cu Kα radiation (λ = 1.5406 A°) with a scan rate of 4° min^{-1}. A continuous scan mode was used to collect 2θ data from 10° to 80°. The composite powders were pressed into 6-mm pellets at 6 MPa and used for conductivity measurements. Conductivity was measured at room temperature by a standard four-probe van der Pauw method. Temperature dependence on DC conductivity was recorded in the temperature range of 30–300 K. The magnetic properties of the samples were measured as a function of the applied magnetic field *H* with a superconducting quantum interference device magnetometer (Quantum Design MPMS-X 1). The hysteresis of the magnetization was obtained with an applied field between +5 kOe and −5 kOe; these measurements were carried out at 300 K.

RESULTS AND DISCUSSION

Synthesis and morphology of Fe_3O_4/SPAN(ANSA) composites.

Preparation of Fe_3O_4/SPAN(ANSA-**A** or **B**)-NCs involves two steps: nanoparticle preparation and

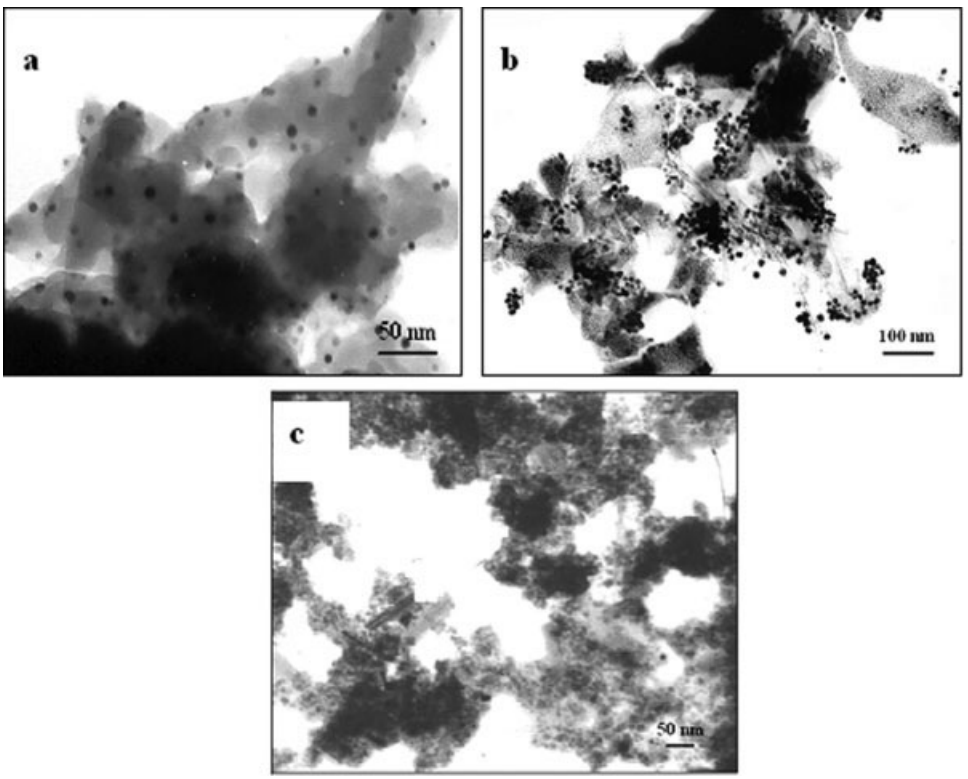

Figure 1 TEM images of (a) Fe_3O_4/SPAN(ANSA-**A**)-NC, (b) Fe_3O_4/SPAN(ANSA-**B**)-NC, and (c) Fe_3O_4 nanoparticles.

composite formation. Fe_3O_4 nanoparticles are formed from coprecipitation of an aqueous solution of iron salts (Fe(II) and Fe(III)) by the addition of ammonia solution (pH $\sim$ 10). The convention Fe(II) and Fe(III) ions to Fe_3O_4 nanoparticles involves through a sequence of complex steps including deprotonation, hydrolysis, oxidation, precipitation, nucleation, crystallization, dehydroxylation, and/or dehydration.[40]

$$Fe^{2+} + 2Fe^{3+} + 8OH^- \longrightarrow Fe(OH)_2 + 2Fe(OH)_3 \longrightarrow Fe_3O_4 + H_2O$$

The combined use of Fe(II) and Fe(III) salts facilitated the packing of iron cations in a spinel structure of Fe_3O_4[41] and negatively charged oxygen ions located on the outermost shell.[41] Precipitation of pure Fe^{3+} ions typically produces amorphous hydrated oxyhydroxide and that can be subsequently converted into Fe_3O_4. Fe_3O_4 phase is stable during the preparation of PANI-Fe_3O_4 composites via oxidative polymerization at low or room temperatures.[37] It is known that Fe_3O_4 oxidizes to α- or γ-forms of Fe_2O_3 under the aeration of hydrosol of Fe_3O_4 at about 100°C.[42,43] The color of the obtained precipitate is black indicating it is Fe_3O_4, whereas the color of Fe_2O_3 is reddish-brown.[42] Upon the addition of APS, the oxidative polymerization of aniline and ANSA proceeds in diluted acidic solution, resulting in encapsulation of SPAN over Fe_3O_4 nanoparticles.

Figure 1 shows the TEM images of Fe_3O_4/SPAN(ANSA-**A** or **B**) nanocomposites [Fig. 1(a,b)] and Fe_3O_4 nanoparticles [Fig. 1(c)]. Fe_3O_4 nanoparticles prepared by the coprecipitation method were highly agglomerated [Fig. 1(c)] probably due to high surface energy and strong dipole–dipole interaction between the nanoparticles.[44] Figure 1(a,b) indicates that Fe_3O_4 nanoparticles of diameters in the ranges 10–15 nm are dispersed homogeneously within the matrix of SPAN. TEM images of the composites [Fig. 1(a,b)] consist of ''gray'' (polymeric) layer over covered ''dark'' Fe_3O_4 nanoparticles (core). The fine dispersion of Fe_3O_4 nanoparticles in the polymer matrix is achieved due to the use of ultrasonication.[45] Ultrasonication prevents the Fe_3O_4 nanoparticles from aggregation and keeps the particles individually in polymer matrix during the polymerization process. SPAN(ANSA-**A** or **B**) presents in the form of a layer over Fe_3O_4 particles probably through electrostatic interactions between positive charges on the surface of Fe_3O_4 nanoparticles and negative charges in sulfonate groups in the SPAN(ANSA). As a consequence, Fe_3O_4 particles are encapsulated through a layer of SPAN-**A** or SPAN-**B**. SEM micrographs of Fe_3O_4/SPAN(ANSA-**A**) and Fe_3O_4/SPAN(ANSA-**B**) compo-

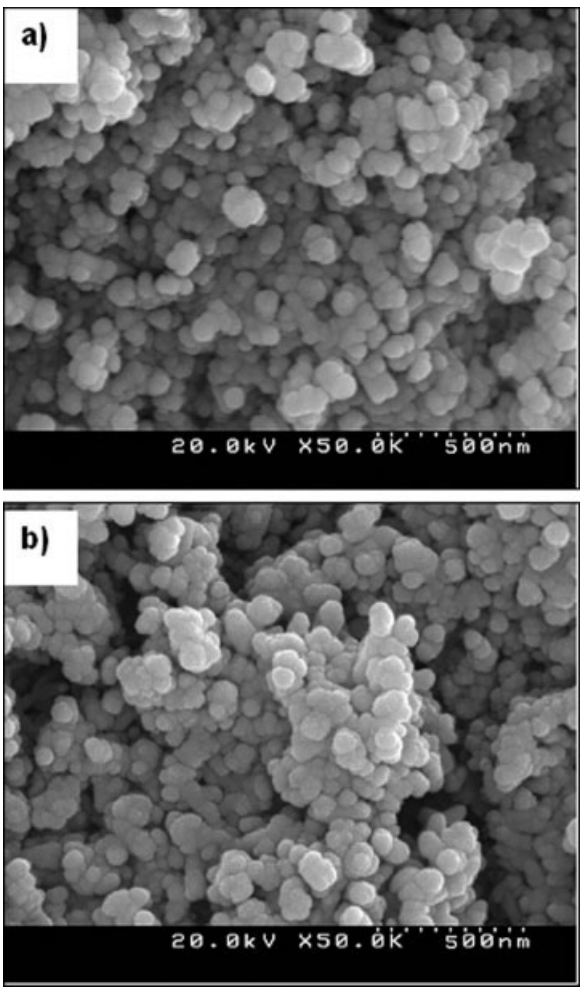

Figure 2 SEM images of (a) Fe_3O_4/SPAN(ANSA-**A**)-NC, and (b) Fe_3O_4/SPAN(ANSA-**B**)-NC.

sites [Fig. 2(a,b)] indicate that the particles are spherical morphology. We anticipate that the incorporation of Fe_3O_4 nanoparticles into SPAN matrix could influence the morphology, thermal, electronic, electrical, and magnetic properties of the resulting composites.

XRD analysis

Figure 3 shows XRD patterns of (a) Fe_3O_4/SPAN(ANSA-**A**)-NC, (b) Fe_3O_4/SPAN(ANSA-**B**)-NC, (c) SPAN(ANSA-**A**), (d) pristine PANI, and (e) Fe_3O_4 nanoparticles. Figure 3(e) clearly shows the Bragg reflections of Fe_3O_4 nanoparticles with 2θ values of 18.32°, 30.35°, 35.7°, 43.44°, 53.82°, 57.31°, 62.89°, 71.02°, and 74.46°. XRD patterns [Fig. 3(e)] confirm that Fe_3O_4 nanoparticles have a cubic spinel structure[46] and in accordance with the joint committee on powder diffraction standards (JCPDS), file No. 19-0629. Diffraction pattern reveals that the Fe_3O_4 particles are having ultrafine size with a single domain structure and they are highly crystalline.[47] The average size of the Fe_3O_4 nanoparticles was estimated from X-ray broadening of the diffraction peaks using Scherrer formula[48] as 18.4 nm (FWHM = 0.44).

Turning to the analysis of XRD patterns of the Fe_3O_4/SPAN(ANSA)-NCs, one can find few additional peaks than observed for the Bragg reflections of Fe_3O_4 nanoparticles and pristine PANI or SPAN. Pristine PANI [Fig. 3(d)] shows diffraction peaks at 2θ = 15.23°, 20.56°, and 25.51°, which are ascribed to the periodicity parallel and perpendicular to the PANI chains, respectively.[49] The peaks of SPAN(ANSA) are comparatively less intense and broader than the peaks of PANI, indicating a more amorphous characteristics for SPAN. And, the broad peak around ~ 15° in PANI was virtually absent in the microstructure of SPAN(ANSA). However, few other new features were noticed in the XRD patterns of Fe_3O_4/SPAN(ANSA)-NCs. Apart from the characteristic peaks of SPAN(ANSA) [Fig. 3(c)], few additional sharp peaks at 2θ = 30.31°, 35.71°, 43.32°, 53.85°, 57.28°, 62.86°, and 73.76° are noticed in the XRD pattern of Fe_3O_4/SPAN(ANSA)-NCs [Fig. 3(a,b)]. The peaks of Fe_3O_4 nanoparticles are present altogether in the composites. It confirms that the coating of polymer on Fe_3O_4 via oxidative polymerization did not result in a phase changes for Fe_3O_4 nanoparticles in the composites. The composites showed improved degree of crystalline order than pristine SPAN(ANSA) and pristine PANI, because of the presence of Fe_3O_4.

Thermal analysis

Thermograms of (a) Fe_3O_4/SPAN(ANSA-**A**), (b) Fe_3O_4/SPAN(ANSA-**B**) composites, (c) SPAN(ANSA-**A**), (d)

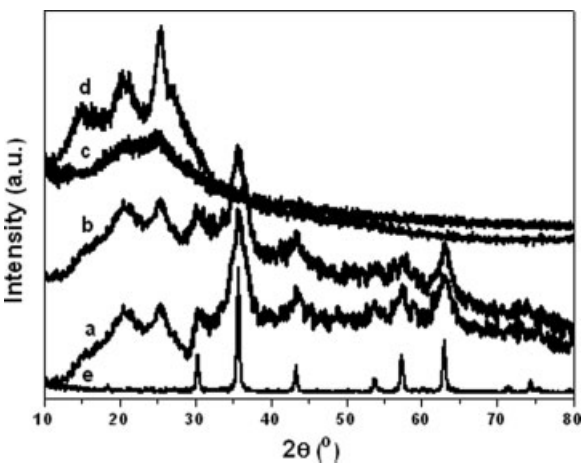

Figure 3 X-ray diffraction pattern of (a) Fe_3O_4/SPAN(ANSA-**A**)-NC, (b) Fe_3O_4/SPAN(ANSA-**B**)-NC, (c) SPAN(ANSA-**A**), (d) pristine PANI, and (e) Fe_3O_4 nanoparticles.

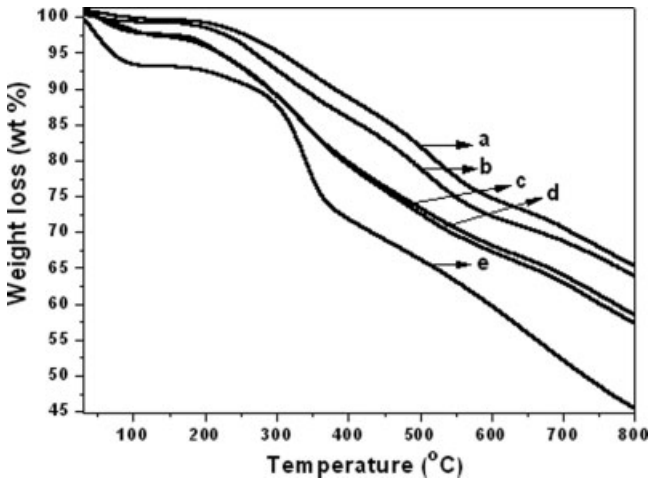

Figure 4 Thermograms of (a) Fe_3O_4/SPAN(ANSA-**A**)-NC, (b) Fe_3O_4/SPAN(ANSA-**B**)-NC, (c) SPAN(ANSA-**A**), (d) SPAN(ANSA-**B**), and (e) pristine PANI.

SPAN(ANSA-**B**), and (e) pristine PANI are presented in Figure 4. The temperature range of 30–800°C is usually sufficient to determine decomposition temperatures of composites and wt % of Fe_3O_4 in the composites.[28,29,34,40,50] Beyond 800°C, significant changes was not observed. PANI or SPAN-ANSA can undergo degradation via two or three steps: expulsion of absorbed water/moisture, decomposition of dopants or SO_3^- units, and decomposition of polymer chains.[36] Fe_3O_4/SPAN(ANSA)-NCs [Fig. 4(a,b)] exhibit better thermal stability than SPAN and pristine PANI. A weight loss of ~ 11% in the temperature between 200 and 400°C was noticed for the composites, whereas for copolymers and PANI, a loss of 17% and 22% mass was observed at the same temperature ranges. The lower weight loss for copolymers (SPAN-ANSA-**A or B**) in comparison to that of pristine PANI is due to the presence of sulfonic groups in the SPANs. Also, ~ 65% of original weight was retained at 800°C for Fe_3O_4/SPAN(ANSA)-NCs [Fig. 4(a,b)], whereas a much lower weight % was retained for SPANs (~ 55%) and pristine PANI (~ 40%).

To carefully compare the thermal behavior of nanocomposites with that of the SPANs, the derivative thermogram (DTG) curves are presented [Fig. 5]. The peaks in DTG curve of pure SPAN(ANSA-**A or B**) [Fig. 5(B)] at 285 and 470°C are attributed to the thermal decomposition of polymer chains. And, thermal decomposition is occurring at higher temperature around 330 and 510°C for Fe_3O_4/SPAN(ANSA-**A or B**) composites [Fig. 5(A)]. This reveals that the temperature of the chain degradation of polymer chains in composites is higher than that of the pristine SPANs, indicating that composites are more thermally stable due to the interaction between groups in SPAN and charges on Fe_3O_4 particles. From TGA analysis, wt % of Fe_3O_4 in the Fe_3O_4/SPAN(ANSA-**A**)-NC and Fe_3O_4/SPAN(ANSA-**B**)-NC are calculated to be 8.73 and 8.21%, respectively.

IR spectra analysis

FTIR spectroscopy was used to understand the molecular interactions between Fe_3O_4 nanoparticles and SPAN(ANSA). At the first instant, the spectral data was used to confirm the formation of copolymer SPAN(ANSA-**A** or **B**). This was done by comparing the spectral characteristics of SPAN(ANSA-**A** or **B**) with pristine PANI. FTIR spectrum [Fig. 6(e)] of PANI has characteristic peaks at 1592 (assigned as C=C stretching of the quinoid rings), 1499 cm^{-1} (C=C stretching deformation of benzenoid ring), 1295 cm^{-1} (C—N stretching of secondary aromatic

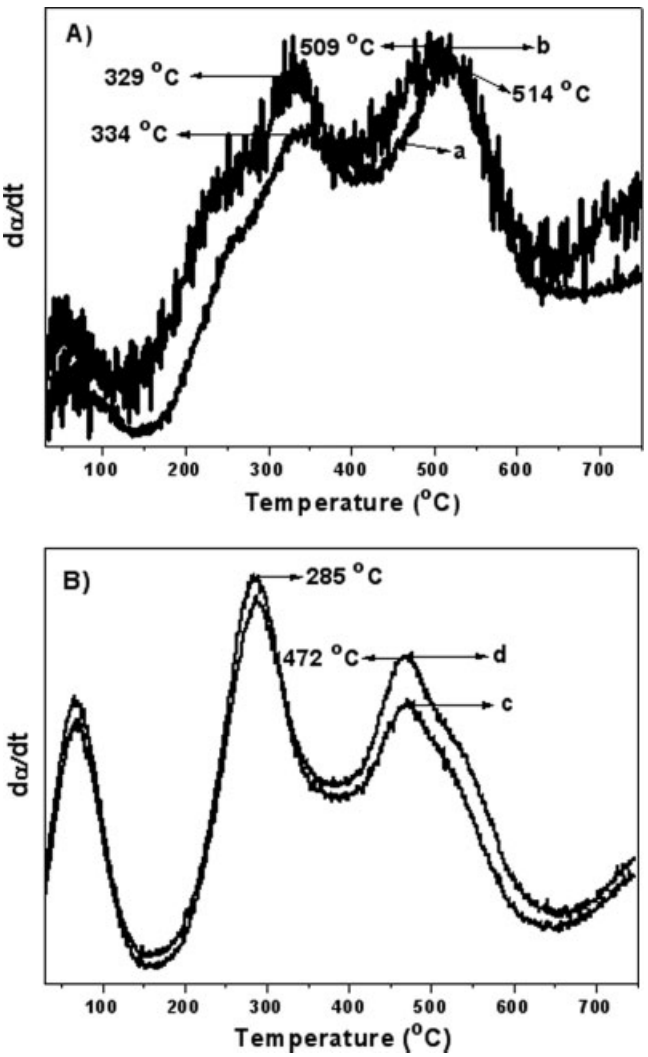

Figure 5 (A) DTG curves of the (a) Fe_3O_4/SPAN(ANSA-**A**)-NC, and (b) Fe_3O_4/SPAN(ANSA-**B**)-NC; (B) DTG curves of the (c) SPAN(ANSA-**A**), and (d) SPAN(ANSA-**B**).

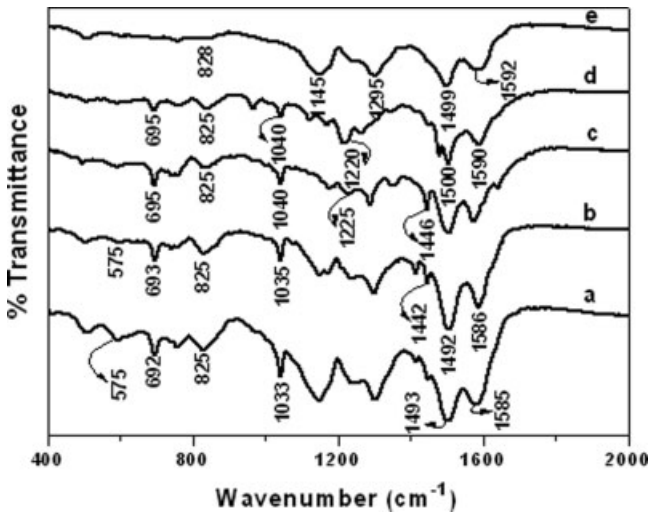

Figure 6 FTIR spectra of (a) Fe_3O_4/SPAN(ANSA-**A**)-NC, (b) Fe_3O_4/SPAN(ANSA-**B**)-NC, (c) SPAN(ANSA-**A**), (d) SPAN(ANSA-**B**), and (e) pristine PANI.

amine), 1145 cm^{-1} (—N=quinoid=N—), and 828 cm^{-1} (out-of-plane deformation C—H in the benzene ring).[51,52] The formation of SPAN [Fig. 6(c,d)] is conformed by the appearance of additional bands near 695, 1040, and 1220 cm^{-1}. The bands at 1240 and 1040 cm^{-1} are attributed to the stretching vibrations of the SO_3 moiety.[53] The intense band at 695 cm^{-1} is due to the C—S aromatic stretching vibration. These bands are present in the spectra of composites [Figs. 6(a,b) and 7(a,b)]. On other hand, the bands at 1590, 1496, 1040, and 695 cm^{-1} observed in the spectrum of the SPAN(ANSA) copolymers are shifted to lower numbers of $\sim$ 5 cm^{-1}, in the spectra of composites [Figs. 6(a,b) and 7(a,b)]. The peak at about 575 cm^{-1} in the spectra of composites are corresponding to Fe—O bond vibration.[54] The peaks observed in the spectra of Fe_3O_4 (inset of Fig. 7) at around 3440 and 575 cm^{-1} are assigned for stretching vibration of absorption of water and Fe—O bond vibration, respectively.[54,55]

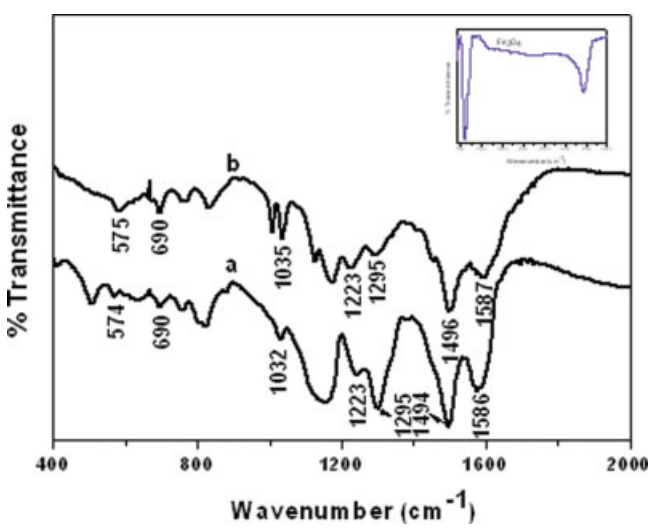

Figure 7 FTIR spectra of (a) Fe_3O_4/SPAN(ANSA-EB-**A**)-NC, (b) Fe_3O_4/SPAN(ANSA-EB-**B**)-NC, and Fe_3O_4 nanoparticles (inset). [Color figure can be viewed in the online issue, which is available at www.interscience.wiley.com.]

UV–vis spectroscopy

UV-vis absorption spectra of Fe_3O_4/SPAN(ANSA) composites, neutralized EB-form of the composites, and pristine PANI are shown in Figure 8. The spectrum of PANI [Fig. 8(e)] has bands around 320 and 620 nm and are assigned for the π-π* and n-π* transitions, respectively.[56,57] The composites show three absorption bands. The additional band appeared around 395 nm in the composites [Fig. 8(a,b)] corresponds to polaronic transitions. EB form of the composites [Figure 8(c,d)] have π-π* and polaronic transitions at 270 and 355 nm, respectively. The shift of bands is caused by interband charge transfer from benzenoid to quinoid moieties of the protonated polymer (polaron/bipolaron transition). It is inferred that doped-form SPAN in Fe_3O_4/SPAN(ANSA-**A** or **B**) composites [Fig. 8(a,b)] is transformed to emerlaldine base form [Fig. 8(c,d)] on treatment with NH_4OH solution.[7] The solution of the Fe_3O_4/SPAN(ANSA-**A** or **B**) composite particles was dark green in color. The color changed from dark green to blue on treatment with NH_4OH solution. Such a color change qualitatively indicates that the doped form of

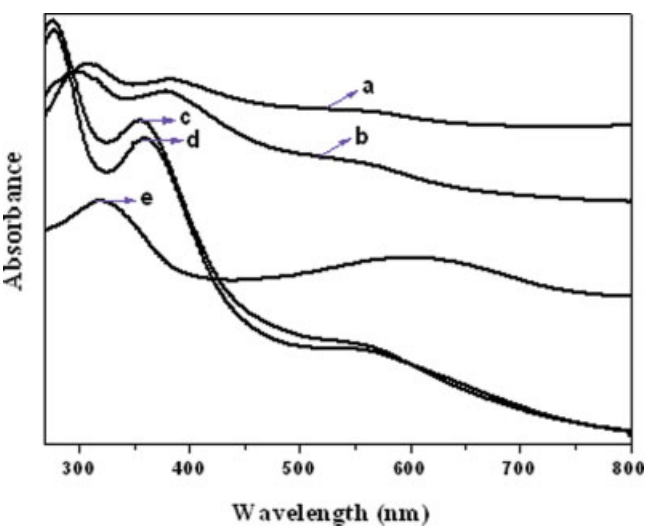

Figure 8 UV–visible spectra of (a) Fe_3O_4/SPAN(ANSA-**A**)-NC, (b) Fe_3O_4/SPAN(ANSA-**B**)-NC, (c) Fe_3O_4/SPAN(ANSA-EB-**A**)-NC, (d) Fe_3O_4/SPAN(ANSA-EB-**B**)-NC, and (e) pristine PANI. [Color figure can be viewed in the online issue, which is available at www.interscience.wiley.com.]

SPAN in the composite is transformed into EB form. This result is consistent with the shifts in bands [Fig. 8(c,d)]. Further, EB form of the composites could be changed into again doped form (green) on treatment with aqueous HCl. This redox reversibility confirms that SPAN in the composite could reversibly undergo protonation–deprotonation changes.

Electrical conductivity

The room temperature electrical conductivity of SPANs and composites was determined using standard four-probe method.[58,59] The room temperature conductivity values of Fe_3O_4/SPAN(ANSA-**A**)-NC and Fe_3O_4/SPAN(ANSA-**B**)-NC are 0.452 and 0.438 S cm^{-1}, respectively. The conductivity of the composites is much higher than that of SPAN(ANSA-**A** or **B**) ($\sim 8.85 \times 10^{-3}$ S cm^{-1}) and pristine PANI (5.19×10^{-3} S cm^{-1}). The additional self-doping possibility contributes to higher conductivity than PANI. The important and interesting observation is that the conductivity of the composites higher over SPAN. Microscopic and macroscopic factors contribute to higher conductivity of the composites. The microscopic conductivity is dependent on doping level, conjugation length, preparation conditions, etc. The macroscopic conductivity is caused by factors such as compactness, crystallinity, size, and morphology of polymer covering on Fe_3O_4 particles. In the composites, a compact layer of SPAN is expected on the surface of Fe_3O_4 nanoparticles. Further, the well-dispersed nature of Fe_3O_4 nanoparticles and the large area of ordered particles provide better contacts between particles. The higher crystallinity of Fe_3O_4/SPAN(ANSA)-NCs as observed with XRD measurements also supports this results. Generally, composite prepared under ultrasonication leads to formation of compact particles in nanoscale with better morphology and contribute to increase in conductivity.[45] We have employed sonication for dispersing nanoparticles in the polymer matrix. The conductivity of the Fe_3O_4/SPAN(ANSA-EB-**A**) and Fe_3O_4/SPAN (ANSA-EB-**B**) is significantly reduced to 10^{-6} S cm^{-1} after treatment with 3 wt % of NH_4OH. This is due to (i) decrease in the doping degree (S/N ratio) from 0.31 to 0.19 after the treatment with NH_4OH solution, (ii) the state of the polymer in the composite was changed to emeraldine base form (EB), which is confirmed by progressive blue shift in adsorption bands in UV-vis spectra of EB-composites.[51] The conductivity of Fe_3O_4/SPAN(ANSA) composites is much higher than reported for the PANI-Fe_3O_4 composite.[27]

The temperature dependence of conductivity of the Fe_3O_4/SPAN(ANSA-**A** or **B**) composites is presented [Fig. 9]. The conductivity values over temperature fit well with ln σ versus $T^{-1/2}$. The DC conductivity of the nanocomposites decreases with decrease in temperature [Fig. 9], indicating typical semiconducting behavior. The variation of conductivity with temperature is usually described by Mott's variable range hopping (VRH) model.[60,61]

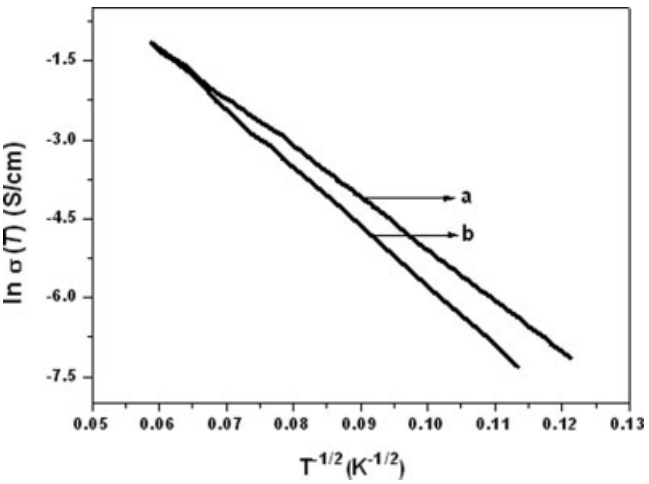

Figure 9 Temperature dependence conductivity of (a) Fe_3O_4/SPAN(ANSA-**A**)-NC, and (b) Fe_3O_4/SPAN(ANSA-**B**)-NC.

$$\sigma(T) = \sigma_0 \exp\left[-\left(\frac{T_o}{T}\right)^{1/f}\right] \quad (1)$$

The exponent f depends on the dimensions of the system. The value of f is 2, 3, and 4 for one, two, and three dimensions. In the one-dimensional (1D) VRH model, eq. (1) can be expressed as

$$\sigma(T) = \sigma_0 \exp\left[-\left(\frac{T_o}{T}\right)^{1/2}\right] \quad (2)$$

where σ_0 is the infinite temperature conductivity and T_o is the effective energy barrier for electrons to hop between localized states and can be written as $T_o = 16/[\alpha^{-1} z N(E_F) k]$, where α^{-1} is the localization length, $N(E_F)$ is the density of states at the Fermi level, k is the Boltzmann constant, and z is the number of nearest-neighboring chains. As shown in Figure 9, the temperature dependence of σ for the both composites is described by the relation $\sigma(T)$ α $\exp[-(T_o/T)^{1/2}]$. The T_o values are estimated from the slopes of the lines in Figure 9. The T_o-values of Fe_3O_4/SPAN(ANSA-**A**) and Fe_3O_4/SPAN(ANSA-**B**) nanocomposites are 9.3×10^3 K and 1.2×10^4 K, respectively.

Magnetic properties

To study the magnetic properties, the as-synthesized fine-powdered samples were filled with gelatin cap-

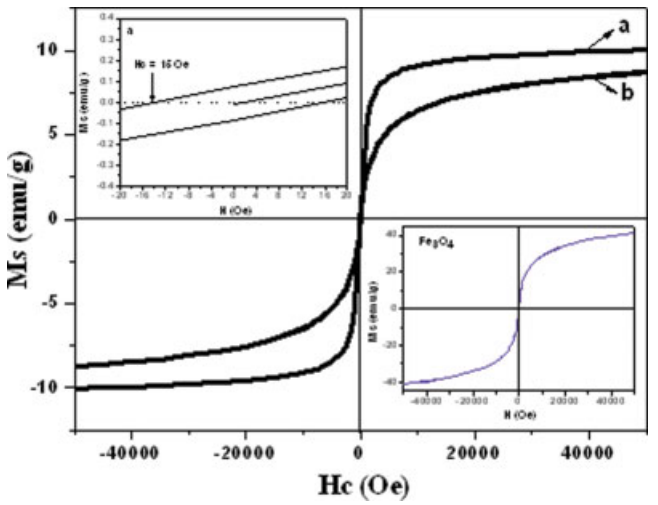

Figure 10 Room-temperature magnetization curves of (a) Fe_3O_4/SPAN(ANSA-**A**)-NC, (b) Fe_3O_4/SPAN(ANSA-**B**)-NC, Fe_3O_4 nanoparticles (right bottom inset), and low magnetic field *M-H* curve of Fe_3O_4/SPAN(ANSA-**A**)-NC (left top inset). [Color figure can be viewed in the online issue, which is available at www.interscience.wiley.com.]

sules that have a small diamagnetic background and the saturation magnetization (M_s) values at 300 K were measured. The plots (*M-H* loop) of magnetization (*M*) versus applied magnetic field (*H*) for (a) Fe_3O_4/SPAN(ANSA-**A**)-NC, (b) Fe_3O_4/SPAN (ANSA-**B**)-NC, and bare Fe_3O_4 nanoparticles (the right bottom inset of Figure) are illustrated in Figure 10. The saturation magnetization of Fe_3O_4 nanoparticles is 44.57 emu g^{-1} (electromagnetic unit per grams), which is lower than that of bulk Fe_3O_4.[62] The lower M_s value for Fe_3O_4 nanoparticles is due to the decrease in particle size and their large surface-to-volume ratio. It is known that the energy of a magnetic particle in an external field is proportional to its size via the number of magnetic molecules in a single magnetic domain. When this energy becomes comparable to the thermal energy, thermal fluctuations will significantly reduce the total magnetic moment at a given field.[63] It is also known that the magnetic molecules on the surface lack complete coordination and the spins are likewise disordered due to their higher surface area.[64] Therefore, M_s value was reduced for Fe_3O_4 nanoparticles.

Fe_3O_4 nanoparticles show ferromagnetic behavior [M_s = 44.57 emu g^{-1}]. It is known that pristine PANI and SPAN are diamagnetic ($M_s \sim -0.03$ emu g^{-1}) at room temperature.[7] Magnetic properties of fine Fe_3O_4 nanoparticles are known to be influenced by the surface modification.[65] From the magnetization curves, we can see that the saturation magnetization (M_s) of Fe_3O_4/SPAN(ANSA-**A**)-NC and Fe_3O_4/SPAN(ANSA-**B**)-NC are 9.782 and 8.865 emu g^{-1}, respectively. Higher M_s values for composites [Fig. 10(a,b)] in comparison to PANI and SPAN(ANSA) is due to the dominant ferromagnetic nature of nanocrystalline Fe_3O_4. The increase in saturation magnetization of composites compared to pure polymers can be attributed to possible charge transfer between the Fe_3O_4 nanoparticle surface and SPAN(ANSA), which changes the electron density, surface anisotropy, crystalline order, and highly oriented magnetization results that affect magnetic properties.[65] Low magnetic field *M-H* curve shows that Fe_3O_4/SPAN(ANSA-**A**) composite (the left top inset of Fig. 10) has coercivity (H_c) of 15 Oe. H_c of bare Fe_3O_4 and Fe_3O_4/SPAN(ANSA-**B**) are 38 and 17 Oe, respectively (Figure not shown). It is known that magnetic surface anisotropy strongly affects the shape of the hysteresis loop and the coercivity.[66,67] This result suggests that composites exhibit ferromagnetic behavior.[29,68] The higher M_s value for Fe_3O_4/SPAN (ANSA-**A**)-NC than for Fe_3O_4/SPAN(ANSA-**B**)-NC is due to the presence of slight excess of Fe_3O_4 content in the Fe_3O_4/SPAN(ANSA-**A**) composite as observed from TGA analysis [Fig. 4(a)]. A high value of magnetization and a low value of coercivity are required for soft magnetic applications. It was found that the magnetic saturation of the composites are not affected on treatment with 3 wt % NH_4OH solution, indicating that M_s values of the composites are independent of the degree of doping. In a simple sense, the Fe_3O_4/SPAN(ANSA-**A/B**) and EB-**A/B** nanocomposites possess ferromagnetic behavior in contrast to diamagnetic behavior of PANI or SPANs.

CONCLUSIONS

Few novel magnetic and conductive composites consisting of a PANI copolymer [SPAN(ANSA)] and Fe_3O_4 nanoparticles were successfully prepared. Fe_3O_4 nanoparticles are coated with a layer of SPAN, and the particles sizes are in the ranges of 10–15 nm. The coexistence of Fe_3O_4 nanoparticles in SPAN(ANSA) significantly influence the thermal stability, crystallinity, electrical conductivity, and magnetic properties of resultant nanocomposites over the pristine polymers. Composites show higher conductivity (0.45 S cm^{-1}) at room temperature than pure PANI and SPANs. The temperature dependence of DC conductivity ($\sigma(T)$) of the composites follows the quasi-1D variable range hopping (quasi-1D VRH) model (i.e., $\sigma(T) \alpha \exp[-(T_o/T)^{1/2}]$). Nanocomposites showed ferromagnetic behavior at 300 K, and Fe_3O_4 was the magnetic phase. Studies regarding the potential applications of this composite material are currently ongoing.

The authors thank the Korean Basic Science Institute (KBSI), Kyungpook National University (KNU), Daegu, for assistance with TEM and XRD analysis.

References

1. Heeger, A. J. J Phys Chem B 2001, 105, 8475.
2. Janata, J.; Josowicz, M. Nat Mater 2003, 2, 19.
3. MacDiarmid, A. G. Angew Chem Int Ed 2001, 40, 2581.
4. MacDiarmid, A. G. Synth Met 2002, 125, 11.
5. Tran, H. D.; Kaner, R. B. Chem Commun 2006, 3915.
6. Skotheim, J. R.; Elsenbaumer, R. L.; Reynolds, J. R. Handbook of Conducting Polymers; Marcel Dekker: New York, 1998.
7. Yue, J.; Wang, Z. H.; Cromack, K. R.; Epstein, A. J.; MacDiarmid, A. G. J Am Chem Soc 1991, 113, 2665.
8. Chevalier, J. W.; Bergeron, J. Y.; Dao, L. H. Macromolecules 1992, 25, 3325.
9. Liu, W.; Kumar, J.; Tripathy, S.; Senecal, K. J.; Samuelson, L. J Am Chem Soc 1999, 121, 71.
10. Salavagione, H. J.; Acevedo, D. F.; Miras, M. C.; Motheo, A. J.; Barbero, C. A. J Polym Sci Part A: Polym Chem 2004, 42, 5587.
11. Abraham, D.; Bharathi, A.; Subramanyam, S. V. Polymer 1996, 37, 5295.
12. Chan, H. S. O.; Neuendorf, A. J.; Ng, S. C.; Wong, P. M. L.; Young, D. J. Chem Commun 1998, 1327.
13. Gangopadhyay, R.; De, A. Chem Mater 2000, 12, 608.
14. Posudeevsky, O. Yu, K. Y. I.; Pokhodenko, V. D. Synth Met 2004, 144, 107.
15. Nalwa, H. S. Encyclopedia of Nanoscience and Nanotechnology, Vol. 2; American Scientific Publishers: Los Angeles, 2004.
16. Fu, G. D.; Zhao, J. P.; Sun, Y. M.; Kang, E. T.; Neoh, K. G. Macromolecules 2007, 40, 2271.
17. Jang, J. Adv Polym Sci 2006, 199, 189.
18. Athawale, A. A.; Bhagwat, S. V. J Appl Polym Sci 2003, 89, 2412.
19. Somani, P. R.; Marimuthu, R.; Sainkar, U. P.; Amalnerkar, D. P. Synth Met 1999, 106, 45.
20. Gurunathan, K.; Trivedi, D. C. Mater Lett 2000, 45, 262.
21. Ficicoglu, F.; Kadirgan, F. Electroanal Chem 1998, 451, 95.
22. Hergt, R.; Hiergeist, R.; Hilger, I.; Kaiser, W. Rec Res Dev Mater Sci 2002, 3, 723.
23. Wang, P. C.; Lee, C. F.; Young, T. H.; Lin, D. T.; Chiu, W. Y. J Polym Sci Part A: Polym Chem 2005, 43, 1342.
24. Gangopadhyay, R.; De, A. Eur Polym J 1985 1999, 35.
25. Butterworth, M. D.; Bell, S. A.; Armes, S. P.; Simpson, A. W. J Colloid Interface Sci 1996, 183, 91.
26. Chen, A.; Wang, H.; Zhao, B.; Wang, J.; Li, X. Acta Mater Compos Sin 2004, 21, 157.
27. Aphesteguy, J. C.; Jacobo, S. E. Physica B 2004, 354, 224.
28. Deng, J. G.; Ding, X. B.; Zhang, W. H.; Peng, Y. X.; Wang, J. H.; Long, X. P.; Li, P.; Chan, A. S. C. Polymer 2002, 43, 2179.
29. Deng, J. G.; He, C. L.; Peng, Y. X.; Wang, J. H.; Long, X. P.; Li, P.; Chan, A. S. C. Synth Met 2003, 139, 295.
30. Liu, G.; Freund, M. S. Macromolecules 1997, 30, 5660.
31. Zhu, Y. G.; Li, Z. Q.; Gu, J. J.; Zhang, D.; Tanimoto, T. J Polym Sci Part B: Polym Phys 2006, 44, 3157.
32. Li, G.; Yan, S.; Zhou, E.; Chen, Y.; Colloids Surf A 2006, 276, 40.
33. Li, L.; Jiang, J.; Xu, F. Eur Polym J 2006, 42, 2221.
34. Li, L.; Jiang, J.; Xu, F. Mater Lett 2007, 61, 1091.
35. Yavuz, O.; Ram, M. K.; Aldissi, M.; Poddar, P.; Hariharan, S. J Mater Chem 2005, 15, 810.
36. Mav, I.; Zigon, M.; Sebenik, A.; Vohlidal, I. J Polym Sci Part A: Polym Chem 2000, 38, 3390.
37. Xia, H.; Cheng, D.; Xiao, C.; Chan, H. S. O. J Mater Chem 2005, 15, 4161.
38. Ding, H.; Wan, M.; Wei, Y. Adv Mater 2007, 19, 465.
39. Zhang, L.; Wan, M.; Wei, Y. Macromol Rapid Commun 2006, 27, 366.
40. Lin, C. L.; Chiu, W. Y. J Polym Sci Part A: Polym Chem 2005, 43, 5923.
41. Kryszewski, M.; Jeszka, J. K. Synth Met 1998, 94, 99.
42. Ziolo, R. F.; Giannelis, E. P.; Weinstein, B. A.; O'Horo, M. P.; Ganguly, B. N.; Mehrotra, V.; Russell, M. W.; Huffman, D. R. Science 1992, 257, 219.
43. Gomez, R.; Hernan, L.; Moralis, J.; Tirado, J. L. Mater Res Bull 1987, 22, 513.
44. Jia, Z.; Wang, Y.; Lu, Y.; Ma, J.; Luo, G. React Funct Polym 2006, 66, 1552.
45. Zhang, Y. P.; Lee, S. H.; Reddy, K. R.; Gopalan, A. I.; Lee, K. P. J Appl Polym Sci 2007, 104, 2743.
46. Sohn, B. H.; Cohen, R. E. Chem Mater 1997, 9, 264.
47. Yang, C.; Guan, Y.; Xing, J.; Liu, J.; Shan, G.; An, Z.; Liu, H. AIChE J 2005, 51, 2011.
48. Klug, H. P.; Alexander, L. E. X.-ray Diffraction Procedures for Polycrystalline and Amorphous Materials; Wiley: New York, 1954.
49. Pouget, J. P.; Jozefowicz, M. E.; Epstein, A. J.; Tang, X.; Macdiarmid, A. G. Macromolecules 1991, 24, 779.
50. Rajan, G. S.; Mauritz, K. A.; Stromeyer, S. L.; Kwee, T.; Mani, P.; Weston, J. L.; Nikles, D. E.; Shamsuzzoha, M. J Polym Sci Part B: Polym Phys 2005, 43, 1475.
51. Oliveira, M. M.; Castro, E. G.; Canestraro, C. D.; Zanchet, D.; Vgarte, D.; Roman, L. S.; Zarbin, A. J. G. J Phys Chem B 2006, 110, 17063.
52. Markovic, M. G.; Matisons, J. G.; Cervini, R.; Simon, G. P.; Fredericks, P. M. Chem Mater 2006, 18, 6258.
53. Nguyen, M. T.; Kasai, P.; Miller, J. L.; Diaz, A. F. Macromolecules 1994, 27, 3625.
54. Cornell, R. M.; Schwertmann, U.; The Iron Oxide: Structure, Properties, Reactions, Occurrence and Uses; Wiley-VCH: Weinheim, New York, 1996.
55. Ma, M.; Zhang, Y.; Yu, W.; Shen, H.-Y.; Zhang, H.-Q.; Gu, N. Colloids Surf A 2003, 212, 219.
56. Huang, W. S.; MacDiarmid, A. G. Polymer 1993, 34, 1833.
57. Reddy, K. R.; Lee, K. P.; Gopalan, A. I.; Kim, M. S.; Showkat, A.; Nho, Y. C. J Polym Sci Part A: Polym Chem 2006, 44, 3355.
58. Jang, J.; Bae, J.; Yoon, S. H. J Mater Chem 2003, 13, 676.
59. Bowler, N.; Huang, Y. Meas Sci Technol 2005, 16, 2193.
60. Mott, N. F.; Davis, E. A. Electronic Processes in Non-Crystalline Materials; Clarendon Press: Oxford, 1979.
61. Wang, Z. H.; Li, C.; Scherr, E. M.; MacDiarmid, A. G.; Epstein, A. J Phys Res Lett 1991, 66, 1745.
62. Zaitsev, V.; Filimonov, D. S.; Presnyakov, I. A.; Gambino, R. J.; Chu, B. J Colloid Interface Sci 1999, 212, 49.
63. Shafi, K. V. P. M.; Gedanken, A.; Prozorov, R.; Balogh, J. Chem Mater 1998, 10, 3445.
64. Chen, D. H.; Wu, S. H. Chem Mater 2000, 12, 1354.
65. Bidan, G.; Jarjayes, O.; Fruchart, J. M.; Hannecart, E. Adv Mater 1994, 6, 152.
66. Jang, J.; Yoon, H. Small 2005, 1, 1195.
67. Reddy, K. R.; Lee, K. P.; Gopalan, A. I. J Nanosci Nanotech 2007, 7, 1.
68. Chen, A.; Wang, H.; Li, X. Synth Met 2004, 145, 153.